Tutor/s
Dra. Maria Sarret Pons
*Department de Ciència de Materials i Química Física*
Dr. Carlos Rodriguez Abreu
*Director del centre QCI*

Grau de Química

# Treball Final de Grau

**Formation of chromonic liquid crystals from dyes and their confinement in water-in-oil and water-in-water emulsions.**

**Formación de cristales líquidos cromónicos a partir de colorantes y su confinamiento en emulsiones agua-en-aceite y agua-en-agua.**

Ramón S. Herrera Restrepo

*June 2019*

UNIVERSITAT DE BARCELONA
B:KC Barcelona Knowledge Campus
Campus d'Excel·lència Internacional

*“Soy de las que piensan que la ciencia tiene una gran belleza. Un científico en su laboratorio no es sólo un técnico: también es un niño colocado ante fenómenos naturales que lo impresionan como un cuento de hadas”.*

Marie Curie

Agradezco al Dr. Carlos Rodríguez por darme la oportunidad de trabajar en su grupo, en un tema de interés personal; por ser paciente ante mis errores y enseñarme como solucionarlos en cada paso del proyecto. A la Dra. Maria Sarret por sus consejos y tiempo dedicado en el desarrollo del trabajo. Al equipo del QCI, que me han dado la mano en momentos de mayor necesidad, para entender las profundidades de un tema desconocido para mí; y en muchos casos por la amistad que se llegó a dar. A mi familia principalmente, que me han ayudado en todos los aspectos para poder culminar esta etapa de mi vida, que han sido pacientes y me han educado para ser la persona que soy hoy en día.

# REPORT

# CONTENTS

# 1. SUMMARY

Chromonics are an interesting class of lyotropic liquid crystals with several potential medical and technological applications. Their confinement in emulsions provides an opportunity to design advanced organic-based materials. In this work, 9 dyes are tested in order to establish chromonic behaviour. Their phases are characterized using Polarized Optical Microscopy and Small Angle X-Ray Scattering (SAXS). Some of them are used for the formulation of stable water-in-oil (W/O) and water-in-water (W/W) emulsions, which are characterized using rheological techniques.

Mesogenic phases were observed in seven of the nine studied dyes. Acid red 27, Alcian blue (chloride and acetate salts), Congo red and Neutral red acetate formed chromonic nematic ($N_c$ phase) and hexagonal (M phase) columnar phases. The structure of their phases was not characterized due to partial insolubility.

The representative chromonic phases are shown through the partial phase diagram of nickel (II) phthalocyanine tetra-sulfonic acid. This compound stacks in cylindrical columns in both $N_c$ and M phases, with a diameter of one molecule.

Two of the studied dyes were used to formulate the emulsion confinement. Representative optical textures of these systems were observed, as star-like and tactoid forms. The chromonic nematic phase of pinacyanol acetate was confined in drops of W/O emulsions with polydimethylsiloxane, vinyldimethylsiloxy terminated as the oil phase. The drop size was highly polydisperse and above 2 μm. This emulsion showed a Newtonian rheology behaviour. Nickel (II) phthalocyanine tetra-sulfonic acid chromonic nematic phase was confined in W/W emulsions with added polyvinylpirrolydone. The W/W emulsion presented a polydisperse drop size larger than 1 μm and showed a Newtonian behaviour. Other oils, surfactants and polymers were tested.

**Keywords**: Emulsion confinement. Lyotropic Chromonic Liquid Crystals. Water-in-water emulsions. Water-in-oil emulsions.

# 2. RESUMEN

Los compuestos cromónicos son cristales líquidos liotrópicos con potenciales aplicaciones médicas y tecnológicas. Su confinamiento en emulsiones permite desarrollar nuevas tecnologías basadas en compuestos orgánicos. En este trabajo se han estudiado 9 colorantes con el fin de establecer la existencia de comportamiento cromónico. Las fases cromónicas han sido identificadas y caracterizadas mediante microscopía óptica de luz polarizada y difracción de rayos X de ángulo pequeño. El confinamiento de algunos de estos compuestos en emulsiones agua-en-aceite y agua-en-agua es investigado y caracterizado mediante reología.

En 7 de los 9 compuestos analizados se observó la formación de fases cromónicas. Las fases cromónicas nemática (fase $N_c$) y hexagonal (fase M) de columnas fueron identificadas para: el Amaranto, azul Alcián (sales de cloruro y acetato), rojo Congo y rojo Neutro. La caracterización de las fases para estos compuestos no pudo llevarse a cabo debido a problemas de solubilidad. En el caso del ácido tetrasulfónico de ftalocianina de níquel (II) se construyó un diagrama de fases parcial, en el cual se indican las respectivas mesofases en función de la concentración y temperatura, estas se componen de moléculas apiladas en forma de columnas cilíndricas.

Dos de los nueve colorantes estudiados fueron confinados en emulsiones, lo cual resultó en la formación de texturas ópticas como cruces de Malta o tactoides. La fase $N_c$ del acetato de pinacianol se confina en gotas de emulsión agua-en-aceite con polidimetilsiloxano terminado en vinil-dimetil-silil como fase oleosa, presentando un comportamiento Newtoniano con gotas de tamaño heterogéneo, superior a las 2 μm. Para el ácido tetrasulfónico de ftalocianina de níquel (II) el confinamiento se realizó en emulsiones agua-en-agua con adición de polivinilpirrolidona. Esta emulsión presentó un comportamiento Newtoniano con gotas de tamaño disperso superior a 1 μm. Se estudiaron otros sistemas cambiando la fase oleosa, el surfactante o el polímero.

**Palabras clave**: Confinamiento en emulsiones. Cristales Líquidos Liotrópicos Cromónicos. Emulsiones agua-en-agua. Emulsiones agua-en-aceite.

# 3. INTRODUCTION

## 3.1. LIQUID CRYSTALS

Substances in a solid state are characterized by having a positional and directional molecular order, i.e. their molecules occupy specific sites in a lattice and point their axes in a specific direction. Meanwhile, molecules do not occupy specific sites in a liquid state and their axes are moving randomly without any specific orientation. Liquid Crystals (LCs) represent a state of matter (a mesophase) between liquid and solid [1,2] (Fig. 1). There, molecules (mesogens) show a short positional range order and are oriented in the same direction, i.e. their phases have a structural order but show liquid mobility [3]. These structural characteristics allow them to form different phases, related to their molecular organization.

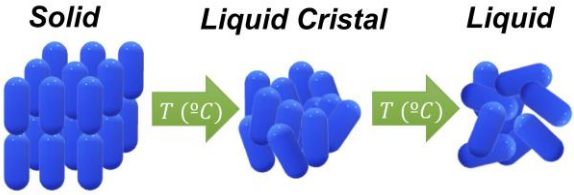


Figure1. Schematic representation of a solid to liquid transition with intermediate LC phase.

LCs can be generally divided into two groups: Thermotropic LCs and Lyotropic LCs. Lyotropic LCs depend on temperature and concentration as they are formed in a solvent, while Thermotropic LCs are only temperature dependent. They are classified as indicated in Figure 2, according to their nature and aggregation, which makes them form different phases. The nematic phase (N phase) only shows orientational order (e.g. Nematic Discotic phase ($N_{Col}$)). The organization of molecules in layers is characteristic of smectic phases (S), which have different conformations depending on their orientation (e.g. smectic A ($S_A$), smectic B ($S_B$) and smectic E ($S_E$) phases) [2]. Some molecules aggregate to form columns, either with orientational order (as in $N_{Col}$) or positional order (as in hexagonal Discotic phase ($Col_h$)) due to their shape. Amphiphilic molecules can, for example, initially form cylindrical micelles, but when concentration is increased a hexagonal arrangement can be achieved (hexagonal Lyotropic phase in $H_1$) [4].

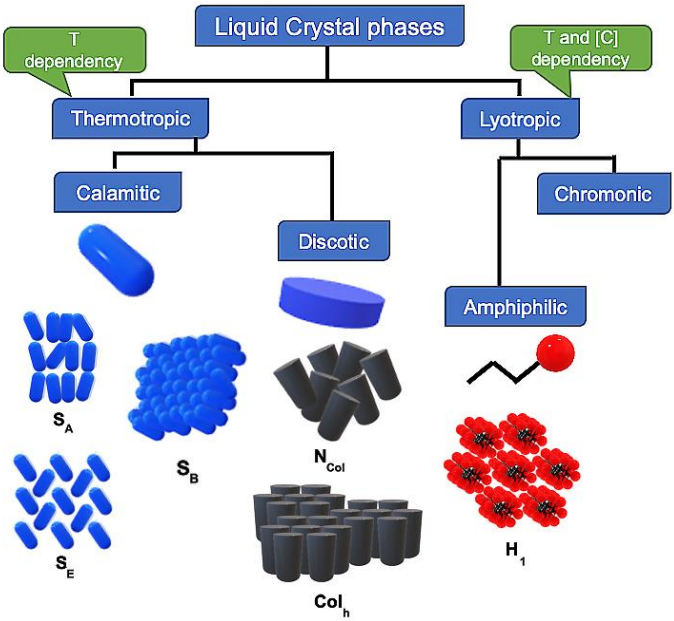


Figure 2. LC types and representative phases.

All these different phases present birefringence, which is an anisotropic optical property (i.e. the light polarization induced by the compound, which presents two different refraction indexes). This allows the identification of the existence of a mesogenic phase and distinguishes between less ordered (as $N_{Col}$ phase) and highly ordered (as $Col_h$) phases. Isotropic (I) solutions do not have any effect on the light transmittance, so they are dark when looked at under the Polarized Optical Microscope (POM), while LCs generate various optical textures related to their phases [4,5].

### 3.1.1. Lyotropic chromonic liquid crystals (LCLCs)

LCLCs (or Chromonics) are formed by rigid, board-like molecules, which have outlying water-soluble groups fixed on an aromatic-nuclei. They are present in dyes, drugs and biologically relevant substances [3,6]. Their $\pi - \pi$ aromatic nuclei interactions allow the stacking in a face to face form between individual molecules, creating a non-polar environment (minimizing their contact with water solvent). This ends in the formation of rigid columns, even in diluted solution [1,3,6] (approx. down $10^{-5}$M [7]). Four to five molecule columns are generally formed as nucleation sites and, when concentrations are increased, the average stacking length increases [7]. The

separation between each stacking board is around 3.4 Å [1,8]. The change of the counter ion (mostly a cation) has a remarkable effect on the formation of chromonics. It can increase solubility and change the transition temperature of the phases at the concentration at which they are observed [3,6,8,9]. These substances can be used to develop new organic base materials, as aligned films, templates, photo-alignment materials, polarizers, biosensors, novel vesicles, etc [6].

The columns can be built in different forms (Fig. 3), having in some cases more than one molecule in the cross-section of the stacking arrangement (e.g. Bordeaux dye has a cross-sectional area equivalent to two molecules [6] (Fig. 3 B)). Chromonics also show brick walls and chimney structures, as in diethylammonium flufenamate and the cyanine dye [3,10–13] (Fig. 3 C and D). These distributions depend on the geometrical relationships between adjacent molecules and the degree of randomness within and between molecules [6].

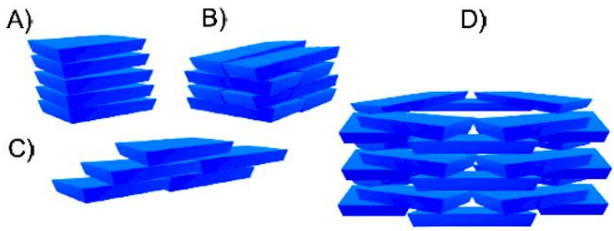


Figure 3. Types of columns. A) Normal stacking. B) Double board width. C) Brick wall representation. D) Chimney representation. Re-drawn from [6].

Chromonic systems mainly show two different phases: The chromonic nematic ($N_c$ phase) and the chromonic hexagonal (M phase) phases. Columns are oriented in the direction of the molecular stacking in the $N_c$ phase, but they do not have any positional order [3]. This mesophase usually occurs at lower concentrations and presents a schlieren defect texture ($N^{Sc}$) produced by a discontinuous orientation of the columns. This defect produces dark threads when aggregates are parallel or perpendicular to the direction of both cross polarizers under POM (Fig. 4) [4,5]. The arrangement is analogous to $N_{Col}$ in discotic systems and $S_A$ phases in calamitic systems [6]. The columns arrange in a regular two-dimensional hexagonal lattice in the M phase [3,6]. A herringbone defect texture ($M^{Hb}$) is observed when the columns, still on an hexagonal arrangement, present a tilt angle when they interact with another layer of columns (Fig. 4) [7].

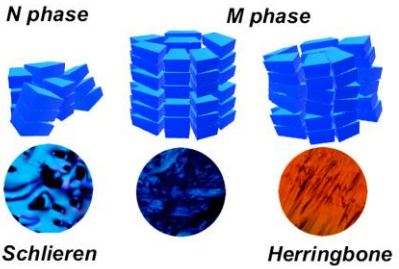


Figure 4. $N_c$ phase and M phase representative textures: Schlieren and Herringbone defects.

Two different dyes, used as reference, will help to identify the existence of chromonic behaviour, as they are well reported nowadays. Disodium cromoglycate (DSCG) (**1**) was the first extensively studied chromonic dye [9]. It is an effective anti-asthmatic drug; a 12 wt% solution shows an $N_c$ phase (Fig. 5) [1]. Sunset yellow (SSY) (**2**) is a dye normally used in the food industry to give yellow-orange colour to products. At a concentration of 30 wt% features an $N_c$ phase at room temperature [1]. Figure 5 shows the representative textures of $N_c$ and M phase in DSCG and SSY aqueous solutions. There, the schlieren and herringbone textures can be seen [6,9].

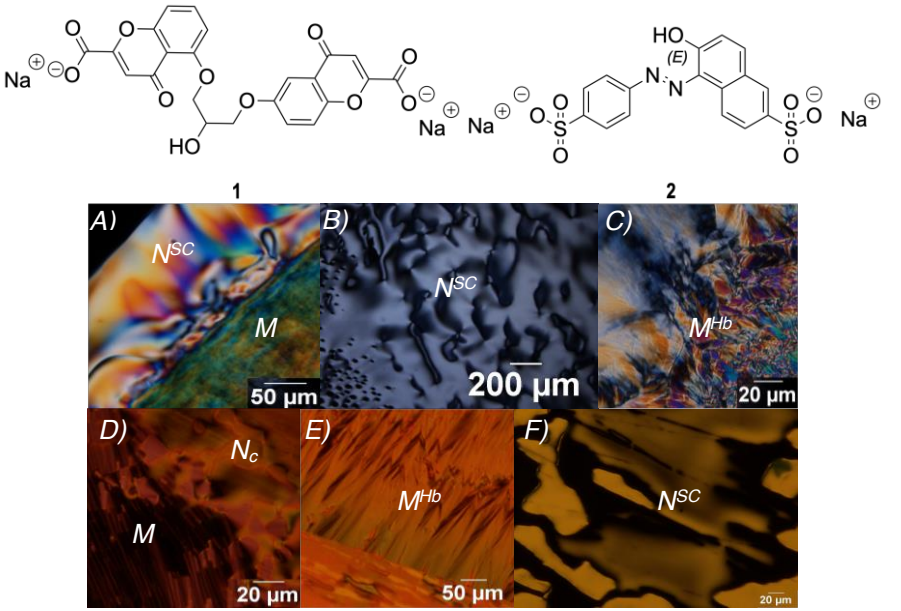


Figure 5. Chemical structures of DSCG (**1**) and SSY (**2**)**.** A), B), C): Optical textures of DSCG. D), E), F): Optical textures of SSY.

### 3.1.2. Small Angle X Ray Scattering (SAXS)

SAXS is a very useful technique to characterize LCs. When X rays impact a sample, electrons become a secondary source of waves that are released in every direction [14]. Samples with a periodic structure are related by the Bragg's equation (Eq.1):

$$n\lambda = 2d\sin(\theta) \qquad \text{Eq. 1}$$

Where $d$ is the distance between planes, $\theta$ is the scattered angle and $\lambda$ is the wave number ($nm^{-1}$) of the incident beam. A peak of constructive waves is produced when the scattering vector ($q$) is plotted versus the measured intensity in the scattering spectrum (Fig. 6), giving structural information on the phase [14]. Then, $q$ is defined by Equation 2:

$$q = \frac{2\pi}{d} \qquad \text{Eq. 2}$$

And Equation 3 is the result of combining Equation 1 and Equation 2:

$$q = \frac{4\pi}{\lambda}\sin(\frac{\theta}{2}) \qquad \text{Eq. 3}$$

The SAXS intensity is the result of different contributions, mainly structural and form factors. Form factors give information about the internal structure, shape and size of the particle; and structure factors give information about interactions within the sample. Samples in this technique do not need to have a crystallographic structure, and even in solution, structural information is obtained. Macromolecules can be analysed by SAXS [14].

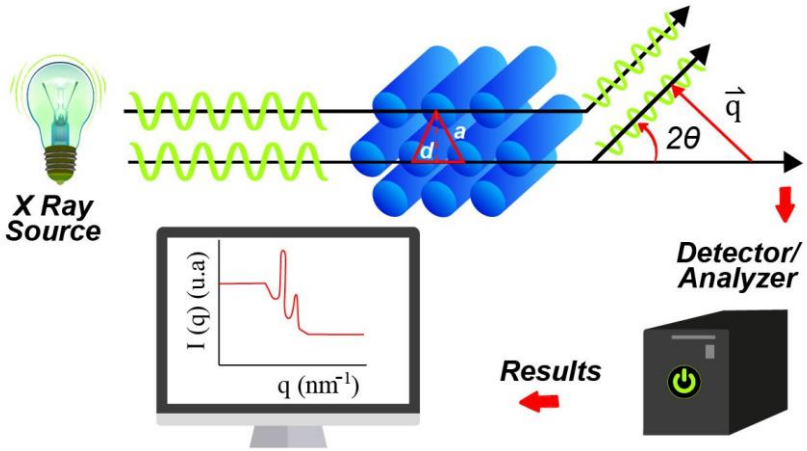


Figure 6. Scheme of SAXS.

LCs usually show periodic distances between 1-100 nm, indicating peaks at low angles. Due to the low positional order in the $N_c$ phase, SAXS peaks are not observed. The M phase, which shows a hexagonal arrangement, will give two or more peaks in a ratio $q_i : q_{i+1}$ of $1 : \sqrt{3} : \sqrt{4} : \sqrt{7}$…. The unit cell parameter $(a)$ for a hexagonal array is defined by Equation 4, which will give the distance between columns [14].

$$a = \frac{2d}{\sqrt{3}} \qquad \text{Eq. 4}$$

## 3.2. EMULSIONS

Emulsions are formed when two immiscible liquid phases are mixed [15]. The dispersed phase is in the form of drops inside the continuous media. The process requires an energy input, mainly due to the size reduction of initial formed drops. The Free Gibbs energy $(\Delta G)$ associated with emulsion formation is defined as in Equation 5:

$$\Delta G = \gamma \, \Delta A \qquad \text{Eq. 5}$$

Where $\gamma$ is the interfacial tension and $\Delta A$ is the increment of the surface area. An increase in the number of drops produces an increment in the $\Delta A$ and $\Delta G$. Drop formation is consequently not spontaneous and emulsions become thermodynamically unstable systems. Stabilization and reduction of the energy cost is achieved by the addition of surfactants, as they reduce the value of the interfacial tension and increase the repulsion between droplets. Solid particles can also be used as emulsion stabilizers [15].

Surfactants are amphiphilic substances that can be characterized by the Hydrophile-Lipophile Balance (HLB) parameter [15]. This parameter was originally defined for ethoxylated non-ionic surfactants as proportional to the weight percent of hydrophilic (ethylene oxide) groups in the molecule. Hydrophobic surfactants have low HLB values (1 to 8 for water-in-oil (W/O) emulsions), whereas hydrophilic surfactants have high values (11 to 50 for Oil-in-water (O/W) emulsions). Surfactants with high HLB are soluble in water, whereas those with low HLB are soluble in oil [15].

Water-in-water (W/W) emulsions are a special case. They are formed by mixing two immiscible aqueous phases, where each phase contains water-soluble macromolecules (non-ionic or ionic polymers or surfactants) that are incompatible in solution by steric factors or salting-out effect [16–18]. Formation of a W/W emulsion implies a phase separation by a segregative mechanism, i.e. the two separated phases contain each of the incompatible macromolecules.

Emulsion pH and ionic strength help to modulate the behaviour of the phases, due to the nature of the polymers [16,17].

Emulsion destabilization can occur by creaming, flocculation, sedimentation, coalescence, phase inversion and Oswald's ripening as shown in Figure 7 [15]. Flocculation is the aggregation of droplets without a change in their volume. The difference in density between the dispersed and continuous phases characterize the cream formation and sedimentation. Denser particles tend to precipitate by gravitational effects, whereas low density drops float over the continuous phase, forming a cream. The formation of larger drops by the junction of small droplets is defined as coalescence, which ends in the separation of the two phases. Phase inversion is the change of W/O to an O/W emulsion, and vice versa. This can be produced by changes in temperature, volume fraction or emulsifier concentration and observed by viscosity and conductivity changes. Oswald's ripening is the formation of bigger drops by the mass transport of the small ones [15].

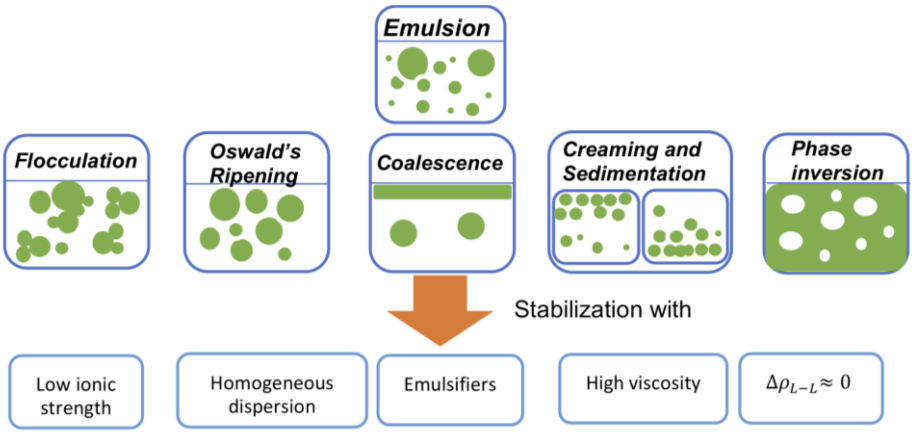


Figure 7. Emulsion destabilization processes.

W/W emulsion differs from the other type of emulsions because it has a lower interfacial tension than those O/W or W/O non-surfactant emulsions. Its instability comes from fast coalescence or flocculation, whereas Oswald ripening is not generally observed [16]. The creaming rate for W/W emulsions is lower than for O/W emulsions, as the density difference of the phases is small [17]. Stabilization of the system can be achieved by the addition of particles that are absorbed on the interface as latex particles, silica or functionalized particles, globular proteins, etc [16].

### 3.2.1. CHROMONIC CONFINEMENT

LCLCs can be confined either in W/O or W/W microscopic emulsions forming ternary systems: Lyotropic Chromonic Liquid Crystal/Oil/Surfactant (LCLC/O/S) or Lyotropic Chromonic Liquid Crystal/Water/Polymer (LCLC/W/P). LCLC/O/S systems allow a versatile study of the behaviour of chromonic systems when confined, as the addition of surfactants helps to control the emulsion properties [19]. In LCLC/W/P systems, where macromolecules induce phase separation, chromonic droplets can be formed [20]. The stabilization of the emulsion and drop morphology depends on different factors, related to the affinity between the emulsifier, the LC phase and the medium (Fig. 8) [20]. For example, DSGC forms stable LCLC/W/P emulsions when mixed with polyvinyl alcohols and polyacrylamides, whereas ionic polymers produce non-stable emulsions with the formation of a precipitate or a LC phase co-existing with an isotropic solution [20]. This confinement may help to design new microstructural materials with biological applications, such as porous materials or vesicles for drug transport.

The confinement induces a different organization of the LCLC columns. This gives the formation of different textures as star-like, tactoid and toroid shape-like (Fig. 8), which are observable with a POM [21].

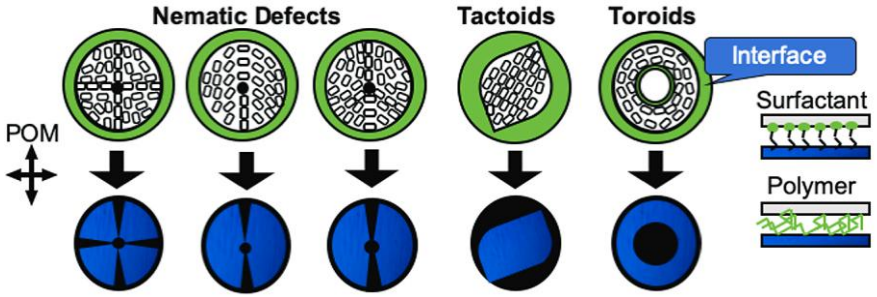


Figure 8. Optical textures of liquid crystals confined in drops.

### 3.2.2. RHEOLOGY

Rheology measurements allow the characterization of emulsions. The dispersed phase, the continuous medium and the emulsifier are the main factors that affect emulsion rheology. Dilute emulsions follow Newton's law (Eq. 6):

$$\sigma = \eta \dot{\gamma} \qquad \text{Eq. 6}$$

Where ($\sigma$) is the shear stress, ($\dot{\gamma}$) is the shear rate and $\eta$ the viscosity. Emulsions generally become non-Newtonian fluids when the dispersed phase concentration is increased, like those indicated in Figure 9. Here, the viscosity is dependent on the shear rate, and the shear stress is defined as [15]:

$$\sigma = \eta_{ap}\ \dot{\gamma}^n = (K\ \dot{\gamma}^{-n})\ \dot{\gamma}^n \qquad \text{Eq. 7}$$

Where $k$ is the consistency index, $n$ is the flow behaviour indexes and $\eta_{ap}$ is the apparent viscosity. If $n$ is equal to 1 in Equation 7, the liquid is Newtonian, above this value is dilatant (shear-thickening) and below 1 is pseudoplastic (shear-thinning) [15].

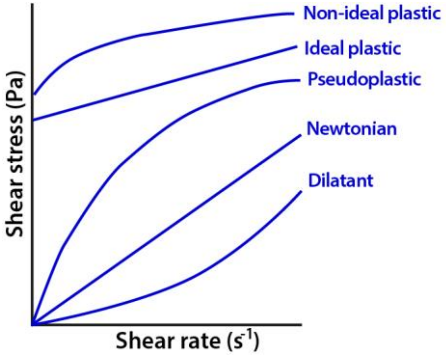


Figure 9. Shear strength $vs$ the shear rate of the stationary liquids.

The organization of droplets in the emulsion under shear stress determines their rheological behaviour. In the case of pseudoplastics (shear-thinning), molecules or particles are oriented in the direction of the flux, so the apparent viscosity is rapidly reduced (they are more likely to flow), whereas in dilatants, where molecules or particles increase their volume, the apparent viscosity is increased with the shear rate (they are less likely to flow). Plastic emulsions need a yield stress before they start to flow. Below this value they behave as an elastic material. This indicates that there is a continuous structure along the systems that restricts the flow at low shear rate values [15].

# 4. OBJECTIVES

Two main objectives are set in this work: First, to establish the occurrence and the characterization of chromonic liquid crystals phases in dye aqueous systems. The effect of counter ion exchange in the chromonic behaviour is studied.

Second, to formulate and characterize stable water-in-oil or water-in-water emulsions with chromonic liquids crystals as the dispersed phase in microscopic confinement.

# 5. EXPERIMENTAL SECTION

## 5.1. MATERIALS AND METHODS

### 5.1.1. Equipment

- Polarized Optical Microscope (POM): BX51TRF-6 Olympus coupled with digital camera Olympus DP73.
- Hot Stage: T95 PE Linkam Scientific Instrument Ltd.
- Small Angle X Ray Scattering (SAXS) instrument: Measurements were carried out using a HECUS X-ray Systems GMBH (Graz, Austria), model S3-Micro. A radiation source ($\lambda$=1.542 Å) from a Cu ($K_\alpha$) anode was used. Scattering was recorded in MBraun PSD-50M and 2D detectors. The generator operated at 1 mA and 50 kV. Temperature was 25 °C controlled by a Peltier device from Anton Paar. Samples are sealed in glass tubes of 80 mm of length, 2.0 mm of diameter with a wall thickness of 0.01 mm.
- Rheometer: AR-G2 Rheometer TA Instruments Ltd coupled with a Peltier-based temperature control.
- Vortex: Vortex- Genier 2/G-560E Scientific industries.
- Ultraturrax T25. Janke & Kunkel Ika-Labortechnik Stauten.
- Freeze Dryer: Alpha 2-4 LD Plus, Martin Christ Gefriertrocknungsanlagen GmbH, coupled with vacuum pump Vaccumbrand RZ6.
- Centrifuge: Eppendorf model 5804 R.

### 5.1.2. Reagents

The reagents use in this work are summarized in the next tables.

| Dye name | Molecular Formula | Supplier | Purity [%] |
|---|---|---|---|
| **Disodium cromoglicate** | $C_{23}H_{14}Na_2O_{11}$ | Alfa Aesar | 98 |
| **Sunset yellow** | $C_{16}H_{10}N_2Na_2O_7S_2$ | Aldrich | 90 |
| **Acid red** | $C_{20}H_{11}N_2Na_3O_{10}S_3$ | TCI | 90 |
| **Indocarbocyanine sodium salt** | $C_{31}H_{39}N_2NaO_6S_2$ | TCI | 98 |
| **Congo red** | $C_{32}H_{22}N_6Na_2O_6S_2$ | TCI | 98 |
| **Neutral red** | $C_{15}H_{17}ClN_4$ | Sigma-Aldrich | 90 |
| **Alcian blue** | $C_{56}H_{40}Cl_4CuN_{12}$ | Sigma-Aldrich | 90 |
| **Pinacyanol acetate** [A] | $C_{27}H_{29}O_2N_2$ | Internal lab. | High |
| **Nickel (II) phthalocyanine tetra-sulfonic acid** | $C_{32}H_{12}N_8Na_4NiO_{12}S_4$ | Aldrich | - |
| **AzBTs** | $C_{18}H_{24}N_6Na_4O_6S_4$ | TCI | 98 |

Table 1. List of dye reagents. ***A.*** Synthetize in the laboratory. IUPAC names are listed in Appendix 1.

| Name | Abbr. | Supplier | Type | HBL |
|---|---|---|---|---|
| **KF6104** | KF-6104 | Shin-Etsu | Surfactant for W/O | Low |
| **Span 80-LQ-(MV)** | Span 80 | Croda | Surfactant for W/O | 4.3 [15] |
| **Hypermer 2296** | Hypermer | Croda | Surfactant W/O | Low |

Table 2. List of Emulsifiers. Structure and name are presented in Appendix 2.

| Name | Abbr. | Supplier | Average mol [$g \cdot mol^{-1}$] |
|---|---|---|---|
| **Polyethylene glycol 4000** | PEG 4000 | ABCR | 3500-4000 |
| **Polyethylene glycol 10000** | PEG 10000 | Sigma | 8500-11500 |
| **Polyvinylpirrolydone K30** | PVP | Aldrich | 40000-80000 |

Table 3. List of polymers. Molecular formula and structure are presented in Appendix 2.

| Name | Abbr. | Supplier | Type | Viscosity [mPa·s] |
|---|---|---|---|---|
| **Polydimethylsiloxane, vinyldimethylsiloxy terminated 0.7 cSt** | PDMS 0.7 | ABCR | Silicone | 0.7 |
| **Polydimethylsiloxane, vinyldimethylsiloxy terminated 200 cSt** | PDMS 200 | ABCR | Silicone | 200 |
| **Squalene** | Squalene | Aldrich | Oil | 28.35-46.35 [22] |
| **Isopropyl myristate** | IPM | Sigma | Oil | 5-4 [23,24] |

Table 4. Lists of oils and hydrophobic media used in the preparation of W/O emulsions.

Silver acetate from Sigma Aldrich and Milli Q water (18.2 M Ω cm) were also used in the experiments.

## 5.2. METHODS

### 5.2.1. Anion exchange

The anion exchange for acetate was carried out with silver acetate in a ratio (1:1.1) for commercial Neutral red chloride salt. First, the substances were weighed and diluted in 10 mL of water and left for 24 hours under stirring, so counter ion exchange is achieved. After this time, the sample was filtered and centrifuged for 30 minutes at 5000 rpm. The supernatant was collected and then lyophilized to eliminate the water solvent.

Alcian blue acetate was prepared in the laboratory applying anion exchange with silver acetate. Commercial Alcian blue (chloride salt) and silver acetate were weighed keeping a molar ratio of 1:4 and diluted in 10 mL of water. It was left for 24 hours under stirring, so counter ion exchange is achieved. After this time, the solution is filtered and centrifuged for 30 minutes at 5000 rpm. The supernatant was collected and then lyophilized to eliminate the water solvent.

### 5.2.2. Testing liquid crystal formation

For the basic contact method, a small quantity of the analyte was deposited over a glass slide and covered with a coverslip. Then, a small droplet of water was put next to the coverslip, so water diffused between the two compartments. The effect is observed with a POM.

For the evaporation contact method, the sample was first completely dissolved in water. Then, a droplet of the solution was deposited over the glass slide and dried in a stove (at approx. 50 ºC). The effect of the water is observed as described in the paragraph above.

### 5.2.3. Preparation of dye aqueous bulk samples

For the basic mixing method, a quantity of the solid dye was dissolved in water and mixed in a vortex with overnight stirring at 50 ºC if it was not completely dissolved. An increase of the sample viscosity is mostly observed. For samples with high viscosity, mixing was achieved by centrifugation through a narrow constriction in glass tubes made in the laboratory. The tubes were flame-sealed after introducing the components.

### 5.2.4. Emulsion preparation

In the case of the W/O emulsions, a solution of the surfactant is prepared in the oil phase, mixing the components in a vortex until complete homogenization. Afterwards, a chromonic aqueous mixture of known concentration was added dropwise upon stirring in a vortex and ultrasonic bath for homogenization. Emulsions were considered stable for characterization if there was no apparent phase separation after 260 minutes.

W/W emulsions were prepared by first dissolving the polymer. Then the solid dye is added at the desired concentration. The mixture is agitated in a vortex for homogenization. High viscous samples are mixed with ultraturrax at mixing speeds between 8000 and 12000 rpm. Samples were mixed using a dispersing tool S25N-10G. Emulsions were considered stable for characterization if there was no apparent phase separation after 260 minutes.

### 5.2.5. Rheology measurements

Steady state flow process was applied to identify rheology behaviour of the prepared emulsions. Measurements have been done at a fixed temperature of 25 ºC with solvent tramp (filled with the correspondent continuous medium), to inhibit solvent evaporation. Standard-size recessed end concentric cylinder and 20 mm steel parallel were used to carry out the measurements.

# 6. RESULTS AND DISCUSSION

## 6.1. PRELIMINARY SCREENING ON THE FORMATION OF CHROMONIC LIQUID CRYSTALS FROM DYES

Figure 10 shows the chemical structure of the 9 tested dyes. Selection was based on previous literature and in their polyaromatic ionic and planar structure that made them candidates for chromonic formation [3,6,8,9]. Acid red 27 (**3**) [25] was used in the test experiments without purification. Alcian blue (**4**) chloride salt was tested as commercial and purified (previously prepared). AzBTs (**5**), Indocarbocyanine sodium salt (**6**) and Congo red (**7**) [26,27] were used without further purification. For Neutral red (**8**) [27] and Alcian blue, anion exchange for acetate was carried out and their acetate salts were tested. Nickel(II) phthalocyanine tetra-sulfonic acid (**9**) [28] was tested as commercial. Pinacyanol is a chloride salt in the commercial form and its anion exchange by an acetate ion (**10**) was previously made in the laboratory.

There are remarkable differences between the structures of the studied dyes. **3**, **5**, **6**, **7**, **8** and **10** dyes have an azo double bound system that joins two parts of the internal aromatic core. The **4** and **9** dyes present a phthalocyanine rigid core coordinated with a metal ion. Their structure is similar to the structure presented in Discotic LCs, so the stacking of molecules in columns should be expected. It is important to notice that the aromaticity of all these compounds helps to keep the structure rigid. The water-soluble groups in the tested molecules consist mainly of sulphate groups, imine or tertiary amines. At working conditions, sulphate groups are ionized (the $pK_a$ of methane-sulfonic acid is -1.8 [29]). The change of the counter ion in **4** acetate salt and **8** might have an effect on the formation of chromonics, as it can change their solubility or affect the transition temperature of their phases [3,6,8,9].

Initially, optical textures under POM help to determine the occurrence of LCLC phases. Preparation of a solution is done to obtain a homogenous phase. If it is achieved, characterization of these phases is done by SAXS technique in later sections.

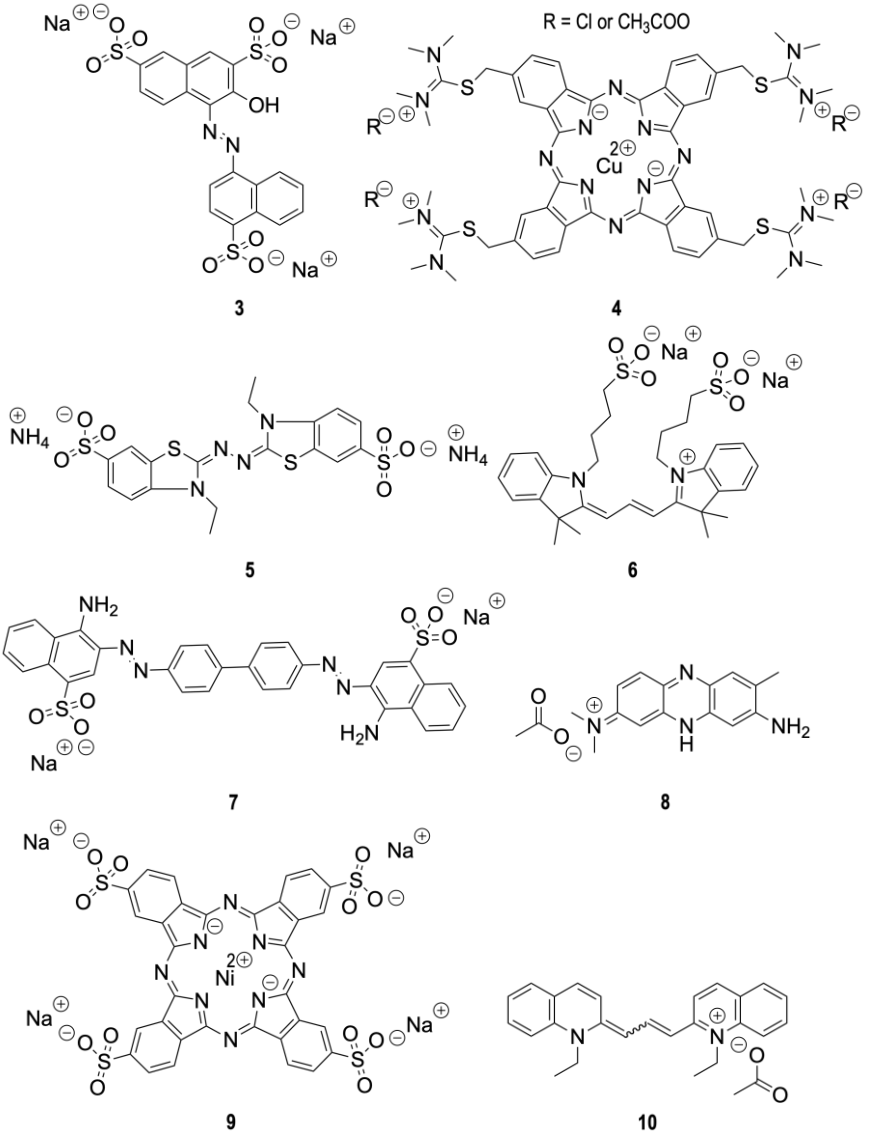


Figure 10. Chemical structure of the tested dyes. **3.** Acid red 27. **4.** Alcian blue (chloride and acetate salt). **5.** AzBTs. **6.** Indocarbocyanine sodium salt. **7.** Congo red. **8.** Neutral red. **9.** Nickel (II) phthalocyanine tetra-sulfonic acid. **10.** Pinacyanol acetate.

### 6.1.1. Acid red 27 (3) and Alcian blue (4)

Using the basic contact method two mesogenic phases ($N_c$ and M) and optic defect textures ($N^{Sc}$ and $M^{Hb}$) for dye **3** were observed (Fig. 11 A and B). Dye solutions were prepared using tubes with a narrow constriction (see experimental section 5.2.3). At a concentration of 5 wt% an isotropic solution was formed. At 20 wt% still no homogeneous mesophase was observed, but the sample presented some rod birefringence particles, probably solid crystals.

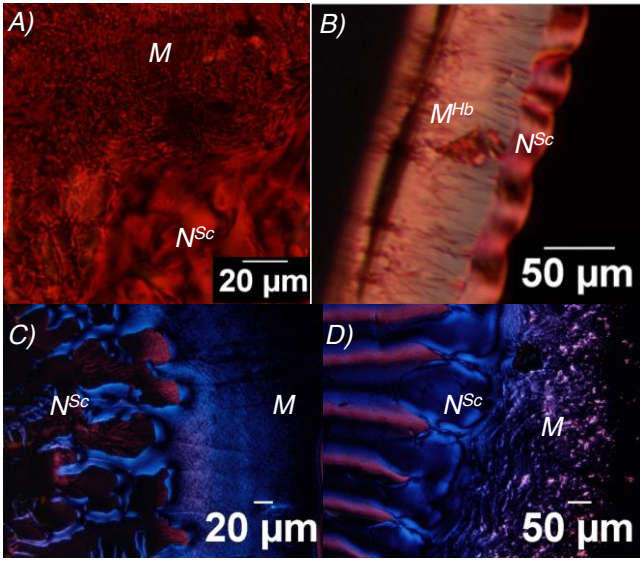


Figure 11. Results of **3**, **4** chloride and **4** acetate. A) Basic contact result of **3**. B) solution at 5 wt% of **3** at the coverslip border. C) **4** acetate basic contact result. D) **4** chloride basic contact result.

Images obtained by the basic contact method are shown in Figure 11 C and D for the **4** chloride and acetate salts. In the case of **4** acetate salt, M and $N_c$ phases were distinguished. When trying to prepare a sample with a fixed concentration, crystals were observed under POM. For **4** chloride salt, the basic contact method allowed the observation of M and $N_c$ phases. A solution was prepared applying the basic mixing method, giving a homogenous $N_c$ phase at 1 wt% of **4** chloride salt.

The presence of solid crystals with the mesophases suggests that there are some impurities in the sample. These do not allow the formation of a homogenous phase when the concentration of the dye is increased. Further purification of the reactant is needed in **3** and in **4** acetate salt.

### 6.1.2. AzBTs (5) and Indocarbocyanine sodium salt (6)

The basic contact method for **5** and **6** showed no formation of mesophases. Instead, they keep a solid crystal shape insoluble in water. **5** clearly showed solid crystals when observed under POM (Fig. 12 A). It is suspected that the ammonium counter ion affects the solubility of the compound. Ammonium ion has similar charge density to cation alkali elements, but a lower hydration number [30,31]. This effect will promote the formation of solid crystals, as the coulombic interaction is not well shielded. Further investigation is needed.

A solution of **6** at 3 wt% was prepared by applying the basic mixing method. No formation of LC texture was observed. The POM/hot stage equipment was used to detect, once melted or dissolved, the mesogenic phases. The solution becomes isotropic between 40-45ºC, without the appearance of LCLCs. Solid crystals formed again when cooled down back to 35 ºC (Fig. 12 B-D). Their formation could be due to the fact that the molecule has its soluble peripherical groups far from the aromatic core, if it is compared with the other studied dyes (**1** and **2**). Then, it is suspected that the hydrophobicity of the compound will stabilize a crystal arrangement, rather than a chromonic phase. Further investigation is needed.

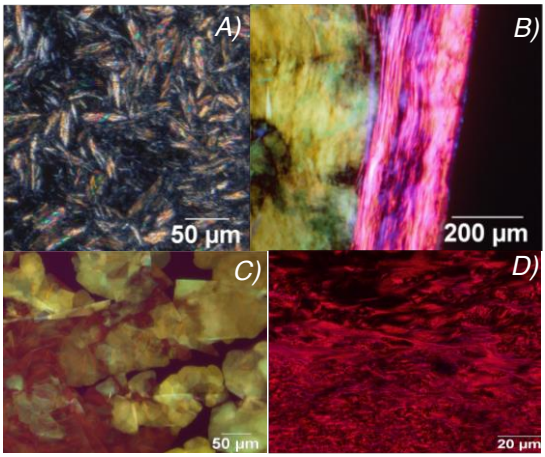


Figure 12. **5** and **6** textures. A) **5** basic contact result. B) Solution at 3 wt% of **6**. C) Phase transition to isotropic solution of **5** D) **6** basic contact result.

### 6.1.3. Congo red (7) and Neutral red (8)

**7** and **8** presented chromonic textures by the basic contact method, but solid crystals were also observed (as in **3** and **4** acetate salt) (Fig. 13). Samples at fixed dye concentration were

made by mixing in tubes with a narrow constriction (see experimental section 5.2.3). **7** showed an M+I biphasic region (i.e. the M phase is in equilibrium with the isotropic phase) of the substance at 5 wt% (Fig. 13 B), but above this value, solid crystals were observed. No single $N_c$ phase was seen when the concentration was decreased. A solution at 20 wt% of **8** was prepared using tubes with a narrow constriction (see experimental section 5.2.3) and next observed applying the evaporation contact method (see experimental section 5.2.2). $N_c$ and M phases could be distinguished, but solid crystals were present. The absence of a single LC phase may be caused by impurities.

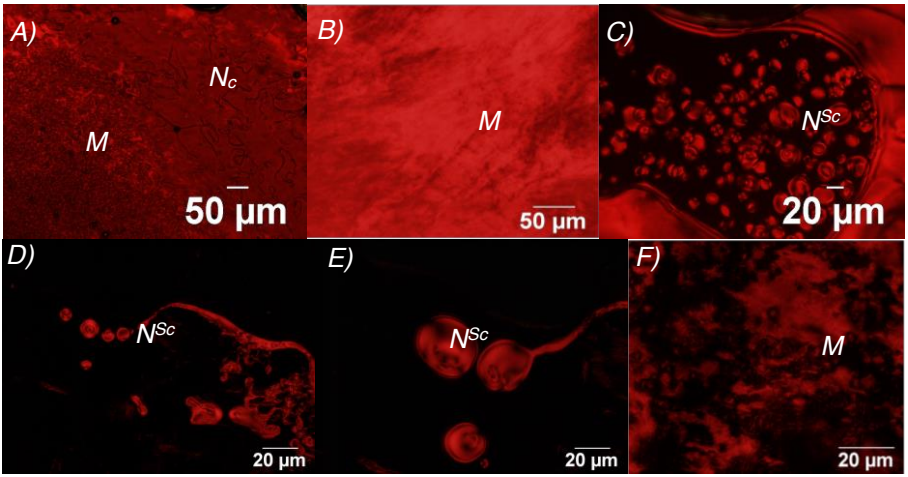


Figure 13. Results of **7** and **8**. A) **7** basic contact result. B) Solution of **7** at 5 wt%. C) **7** $N_c$ phase. D), E): $N_c$ phase, F) M phase of **8.**

### 6.1.4. Nickel (II) phthalocyanine tetra-sulfonic acid (9) and Pinacyanol acetate (10)

**9** is highly soluble in water and presents mesophases on a reasonable range of concentrations. The basic contact method showed the existence of the $N_c$ and M phases, which are presented in Figure 14 A-C. The solution preparation was done applying the basic mixing method (see experimental section 5.2.2), obtaining an $N_c$ phase between 20-25 wt% (Fig. 14 C) and an M phase (Fig. 14 B) at 29 wt%. Partial phase diagram and structure analysis are presented in the next section.

**10** was prepared and purified in the laboratory before being used. The basic contact method showed the $N_c$ and M phase (Fig. 14 D and E). The basic mixing method was used to prepare a

solution at 3 wt%, which showed a homogeneous $N_c$ phase (Fig. 14 F). A chimney structure was already identified by Carlos Rodriguez [32]. Structure analysis is presented in the next section.

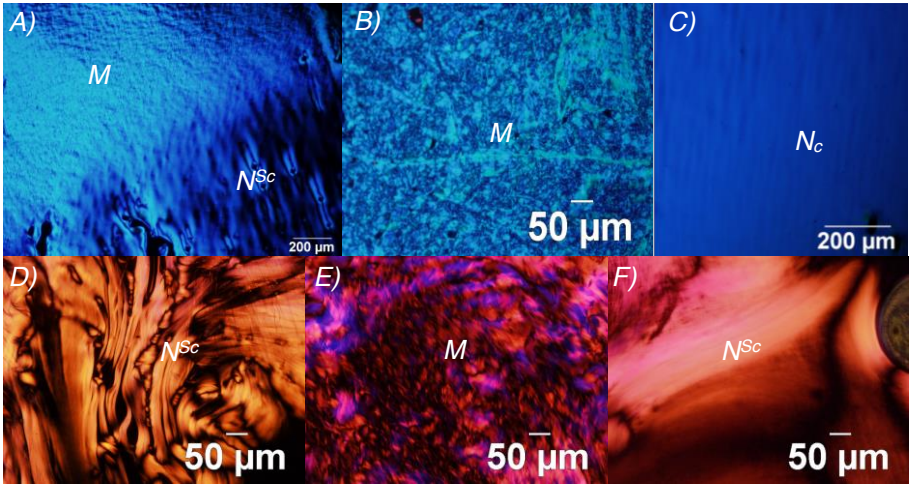


Figure 14. Results of **9** and **10**. A) Basic contact result, B) M phase and C) $N_c$ phase of **9**. D) $N_c$ phase, E) M phase and F) solution at 3 wt% of **10**.

## 6.2. PHASE BEHAVIOUR AND STRUCTURE OF LCLC OF NICKEL (II) PHTHALOCYANINE TETRA-SULFONIC ACID (9) AND PINACYANOL ACETATE (10)

### 6.2.1. Nickel (II) phthalocyanine tetra-sulfonic acid (9)

The partial phase diagram of **9** (Fig. 15) was built using POM/Hot Stage equipment and varying the concentration between 14 wt% and 29 wt%. The coverslip and slide were sealed with glue to avoid water evaporation. At room temperature (25 ºC) a homogeneous $N_c$ phase between 20-25 wt% and an M phase above 29 wt% were observed. An $N_c$+M biphasic region (i.e. the $N_c$ phase in equilibrium with the M phase) is present between 25-29 wt% and an $N_c$+I biphasic region at concentrations lower than 20 wt%. Isotropic (non-birefringent) solutions are obtained below 14 wt%. When the temperature was increased at 30 wt%, a non-isotropic phase was obtained. An isotropic phase was only formed with heat (transition between 80-85 ºC) at concentrations below than 24 wt%. Even at 27 wt%, at temperatures above 90 ºC, $N_c$+I biphasic region was observed. At 20 wt% isotropic phases are formed at 60-65 ºC. These high temperatures of isotropic transition suggest high stability of the columns in both $N_c$ and M phases, i.e. a high input of energy is needed

to disorder them. The phase diagram of **1** in [7] shows that its transition temperatures of chromonic phases are lower, if they are compared with the values obtained here.

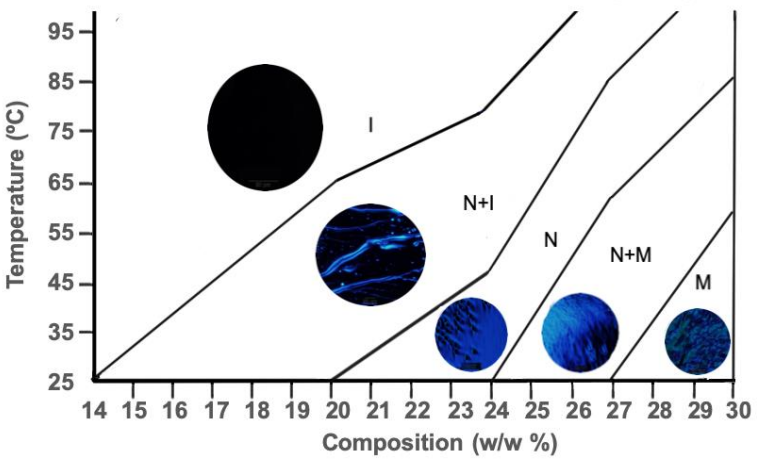


Figure 15. Partial phase diagram of **9** in water.

The characterization of LCLC phases for **9** was carried out by SAXS measurements. At 29 wt% two peaks were observed (Fig. 16) with a ratio $q_1 : q_2$ of 1:1.76 (which is almost 1:$\sqrt{3}$ typical of hexagonal structures). The $q$ value of the first peak is 2.86 nm$^{-1}$, corresponding to an interlayer distance of 2.2 nm (Eq. 2). The "$a$" cell parameter is 2.5 nm (Eq. 4). The radius of the columns ($R$) in the hexagonal phase is calculated by Equation 8 [33]:

$$R = \left\{\left[2\phi_L/\sqrt{3}\pi\right]^{1/2} d\right\} \quad \text{Eq. 8}$$

Where the interlayer distance is $d$ and the volume fraction is $\phi_L$ (Eq. 9):

$$\phi_L = V_{LCLC}/(V_{LCLC} + V_{H_2O}) \quad \text{Eq. 9}$$

Where $V_{LCLC}$ is the volume of **9** in the solution and $V_{H_2O}$ is the volume of Milli Q water. These values are calculated from their density and weighted quantity. Here, only the size of the phthalocyanine core is considered, without the peripherical ionic groups. The density of **9** is taken from the literature (approx. the phthalocyanine value of 1.5 g/mL [34]), giving a value of volumn fraction: $\phi_L = 0.23$, and a column radius: $R = 0.6$ nm. Therefore, a column diameter of 1.2 nm is obtained. The size of the phthalocyanine core of **9** measured on ChemDraw and reported in [35] is 1.4-1.5 nm. These indicates that the columns have approximately the size of one molecule as cross-section and no brick walls or chimney structures are found.

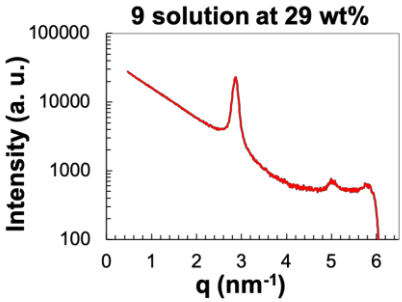


Figure 16. SAXS results of **9** M phase in water at 25ºC.

The SAXS curve of $N_c$ phase at 24 wt% (Fig. 17) was fitted using the Sasfit programme developed by Joachim Kohlbrecher and Ingo Bressler [36]. For data treatment, the water signal contribution was subtracted. Data were fitted to the model of a cylinder of radius ($R$), length ($L$) and scattering contrast ($\Delta n$), according to Equation 10 [36]:

$$I_{Cyl} = 16(\pi R^2 L \Delta n)^2 \int_0^1 \left(J_1\left(qR\sqrt{1-x^2}\right)\sin\left(\frac{QLx}{2}\right)/q^2\, R\,\sqrt{1-x^2}Lx\right)^2 dx \qquad \text{Eq. 10}$$

Where $q$ is the scattering vector and $J_1$ is the regular cylindrical Bessel function of first order [36]. The $N_c$ phase of **9** at 24 wt%, with a $\Delta n$ of 3.5x10$^{-4}$ nm$^{-2}$ and a Gaussian distribution of the column length, gave a cross-section radius of 1.1 nm, which is larger than that obtained in the M phase. This can be attributed to the contribution of charged peripheral groups (including hydration), which are not considered in the calculations for the M phase. The average length of the columns is 1.6 nm with a standard deviation of 0.5 nm and the number of molecules per aggregates is 3 to 6. These values are obtained assuming a spacing between stacking molecules of 0.34 nm.

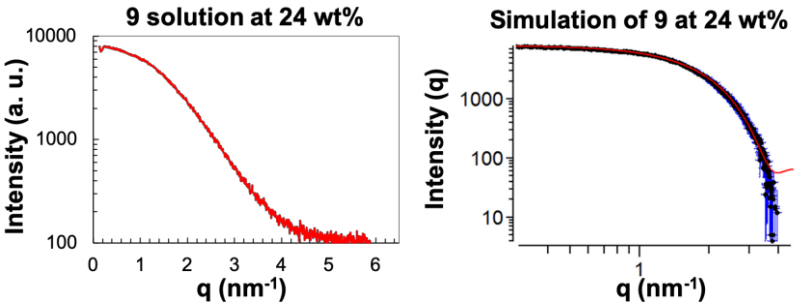


Figure 17. SAXS results and simulation of **9** $N_c$ phase in water at 25ºC.

### 6.2.2. Pinacyanol acetate

Figure 18 shows SAXS result for the $N_c$ phase of **10**. The structure consists of long hollow aggregates. The diameter of the tube is 4.6 nm with a middle wall of 0.3 nm corresponding to the molecular size of the quinaldine moiety. 8 molecules conform the cross-section, having their acetate groups in the inner and outer regions of the cylinder. The deep minima observed in the spectrum indicates low size polydispersity [32].

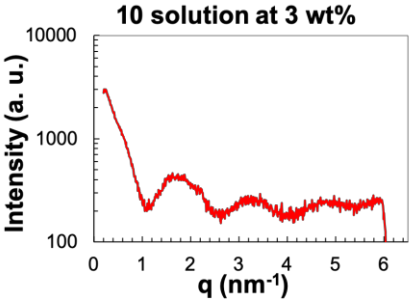


Figure 18. SAXS results of **10** in water at 3 wt%.

## 6.3. FORMULATION AND CHARACTERIZATION OF LCLC EMULSIONS

### 6.3.1 Water-in-oil (W/O) emulsions

The formulation study of LCLC confined in emulsions was focused on **9** solution at 24 wt% and **10** solution at 3 wt%, which showed a homogenous $N_c$ phase. Although solutions of **2** and **4** were also explored, experiments were not successful. Formulations of LCLC/O/S emulsions are summarized in Tables 5 and Table 6. LCLC solution is always at a concentration of 5 wt% in the emulsion. Several oils and surfactants (emulsifiers) were tested.

| Sample | Composition [mass ratios] | Emulsion stability |
|---|---|---|
| **T51** | **LCLC/Squalene/Hypermer =** 5/80/15 | Poor. |
| **T52** | **LCLC/Squalene/Span 80 =** 5/75/20 | Poor. |
| **T53** | **LCLC/Squalene/Hypermer =** 5/75/20 | Poor. |
| **T54** | **LCLC/PDMS 200/KF6104 =** 5/75/20 | Poor. |
| **T55** | **LCLC/IPM/Span 80 =** 5/80/15 | Poor. |

Table 5. LCLC/O/S emulsions of **9** solution at 24 wt%.

The $N_c$ phase of **9** is present between 20 and 24 wt%, but emulsions with **9** at 20 wt% showed drops with no birefringence, so finally emulsions were prepared with **9** at 24 wt%. **T51** emulsion drops are shown in Figure 19 A, which presented poor stability. This did not improve with an increase in the viscosity of the continuous medium. The number of birefringent drops was reduced when the surfactant concentration was increased to 20 wt%, but its shape was more homogeneous and optical textures were improved in **T53** (Fig. 19 B). However, the emulsion still showed the formation of a precipitate and low stability. This indicates a fast destabilization coalescence process, and no stable emulsion was produced with this surfactant. Also, interactions between the oil phase and the chromonic phase might induce the precipitation rather than the formation of drops. Emulsion formed with the surfactant Span 80 (**T52**) did not have good stability and the formation of a blue precipitate on the walls was observed as well. Nevertheless, drops were identified (Fig. 19 C). To improve the emulsion stability a PDMS with kinematic viscosity of 200 cSt was used to produce **T54**. The stability increased as expected, but still was not enough to be measured by rheology. Ultraturrax was used to make this last emulsion. Drops are shown in Figure 19 D. The drops were surrounded by some agglomeration (which was drop-shaped), suggesting flocculation in the sample as a destabilization process. These formulations indicate that the surfactants and oils used to formulate the **9**/O/S emulsions, present some interaction with the chromonic phase, inducing the destabilization and separation of the phases.

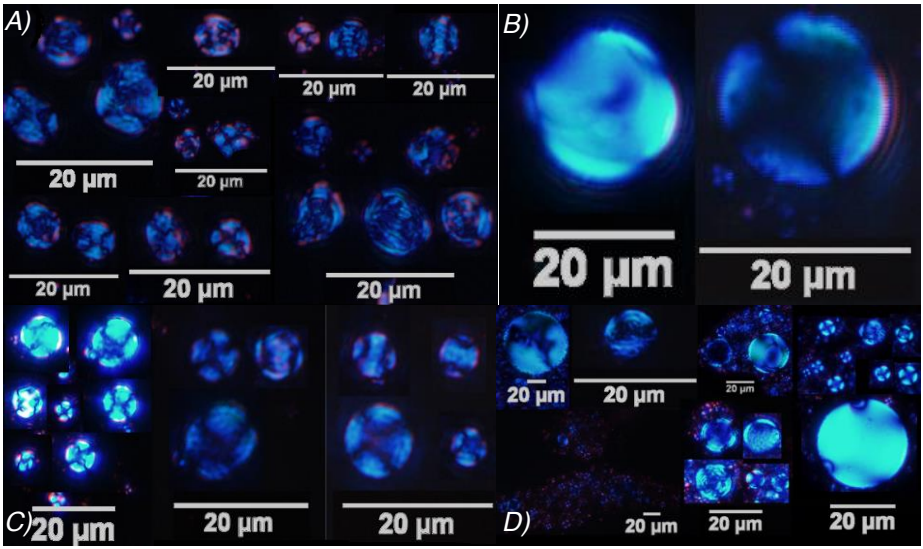


Figure 19. Images of **9**/O/S emulsions. A) **T51**, B) **T53**, C) **T52** and D) **T54** emulsions.

Well defined chromonic nematic drops were obtained in most of the **9**/O/S formulations. **9** columns self-organize in different manners as in Figure 8. Schlieren threads in drops are organized in a cross-like or star-like shape, starting from the centre of the drop. Columns are distributed randomly or are parallel or perpendicular to the direction of the cross polarisers along the threads. The organization of columns in these zones made birefringence occur at lower concentrations inside the drops. Blue and purple drops were observed, which can be related to the dependence of birefringence with the organization of the columns and LC defects [2,19,21]. Drops also showed a $N^{Sc}$ texture.

| Sample | Composition [mass ratios] | Emulsion stability |
|---|---|---|
| **T61** | **LCLC/PDMS 0.7 /KF6104 =** 5/80/15 | Poor. |
| **T62** | **LCLC/PDMS 0.7/KF6104 =** 4/79/17 | Good |
| **T63** | **LCLC/PDMS 0.7/KF6104 =** 2.5/88/9.5 | Good |
| **T64** | **LCLC/PDMS 0.7/KF6104 =** 5/85/10 | Good |
| **T65** | **LCLC/Squalene/Span 80 =** 5/80/15 | Poor. |
| **T66** | **LCLC/IPM/Span 80 =** 5/80/15 | Poor. |

Table 6. LCLC/O/S emulsions of **10** solution at 3 wt%.

Emulsion **T61** showed at first highly stable big drops without the need of strong agitation (Fig. 20 A). Stronger agitation with ultrasonication, led to a reduction of the drop size, allowing the observation of representative confinement textures (Fig. 20 B and C). However, **T61** was unstable. The stability increased when the concentration of surfactant was 17 wt%.

Dilution of an emulsion of **10** solution at 3 wt%/PDMS 0.7 cSt/KF6104, with a 5/75/20 mass ratio, was made to form **T63**. Concentration of **10** (solution at 3 wt% in water) was increased until 5 wt% in **T64**. Then surfactant concentration was increased until 17 wt% to give **T62**. Rheology measurements of **T62**, **T63** and **T64** were carried out using concentric cylinders. Two replicates were measured for each emulsion, leaving a 30-minute rest between replicas. **T62** was measured two times, with a difference of four days. **T62** was mixed again to form an emulsion after the four days due to the poor stability (i.e. the emulsion showed coalescence by forming a dark precipitate at the bottom of the vial). Drops can be observed in Figure 20 B and C.

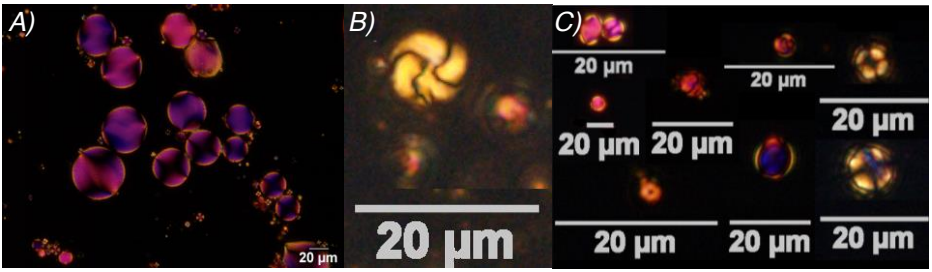


Figure 20. **10** solution at 3 wt% /PDMS 0.7 cSt/KF6104 emulsion images. A) **T61** emulsion. B), C): collage of drops in emulsions **T62-T64**.

Rheology results are shown in Figure 21. The PDMS 0.7, **T62**, **T63** and **T64** presented Newtonian behaviour, which indicates the formation of diluted emulsions in **T62-T64**. PDMS 0.7 has an apparent dynamic viscosity of 0.6 mPa·s equivalent to a kinematic viscosity of 0.74 cSt (the reported value by the manufacturer is 0.7 cSt and a density of 0.810 g·mL$^{-1}$). The difference could be due to experimental factors. This viscosity is calculated as the mean value of each measured point, as it does not change with the shear rate. The formation of the emulsion makes the viscosity increase in **T62**, **T63** and **T64**. A slightly increase is produced when the disperse phase is at 5 wt% in **T64**. A higher increment is produced when the surfactant concentration is 17 wt% (if it is compared **T63** with the PDMS 0.7, and **T62** with the other formulations). This reveals a higher dependence on the surfactant concentration in the stability and viscosity. The rheology behaviour is not affected at the worked compositions by concentration changes in the surfactant and in the dispersed phase. No changes were observed after measurements at different days.

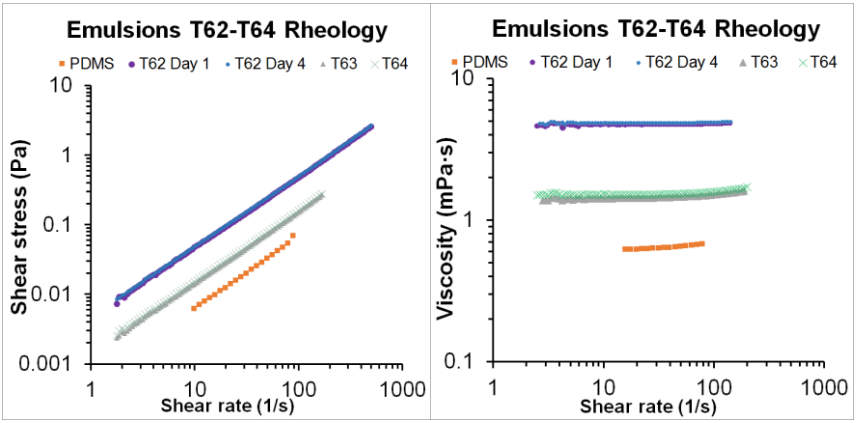


Figure 21. Rheology results of **T62-T64** emulsions.

The stability of **T65** did not improve with an increase of the viscosity of the continuous media (see Table 4). The destabilization of the system leaves a white-violet precipitate on the bottom of the vial, which could indicate sedimentation or coalescence destabilization by interaction with the surfactant. Even so, stable drops can be seen under POM, as shown in Figure 22. Chromonic nematic textures are seen, although under these conditions the number of drops was small and most of them presented a big size compared with **T62**. Mixing of the sample is difficult and ultraturrax is needed.

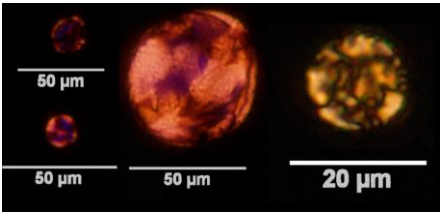


Figure 22. **T65** emulsion drops.

Emulsions formulated with Isopropyl myristate (**T66** and **T55**) were unstable, and a precipitate was instantly formed in the case of **T55** and after a few minutes on **T66**. It suggests that in this environment, the interface between the LCLC and the media does not produce stable emulsion, even if the interfacial tension is reduced with Span 80.

### 6.3.2 Water-in-Water emulsions

Table 7 summarizes the stability of the studied LCLC/Water/Polymer systems with different polymers. No emulsions were formed with PEG in any of the cases, even when the molecular weight of the polymer was increased [16]. Coexisiting $N_c$+I phases were observed by POM, without the formation of any drops similar to those found in DSCG/water/polyanions emulsions [20]. The interaction between the polymer and the LCLC seems to be favourable, so the polymer mixes with the mesogenic phase.

| Sample | Polymer solution [wt%] | 10 solution [3 wt%] | 9 solution [24 wt%] |
|---|---|---|---|
| **T71** | **PEG 4000 (**10**)** | No emulsion formation | No emulsion formation |
| **T72** | **PEG 10000 (**10**)** | No emulsion formation | No emulsion formation |
| **T73** | **PVP (**4**)** | No emulsion formation | Emulsion with high stability |

Table 7. Stability of LCLC/W/P emulsions.

The **T73** samples containing **10** showed the same negative results as with **T71** and **T72**. In contrast, **T73** sample with **9** resulted in a highly stable LCLC/W/P emulsion (Fig. 23 A). The formulation corresponds to a composition (in mass ratios) of **9**/Water/PVP (19.9/76.2/3.9). An increment in the concentration of PVP leads to the formation of threads in the solution above 4 wt%. Reducing the concentration of **9** to 17 wt% induces the loss of birefringence and no emulsion is formed. Drops were observed for more than 6 days and even with centrifugation, phase separation was hard to achieve. The emulsion had a high size polydispersity, nevertheless it was kinetically stable. Tactoid forms were also observed, but no toroid forms (Fig. 23 B) [19]. Drops textures correspond to schlieren star-like.

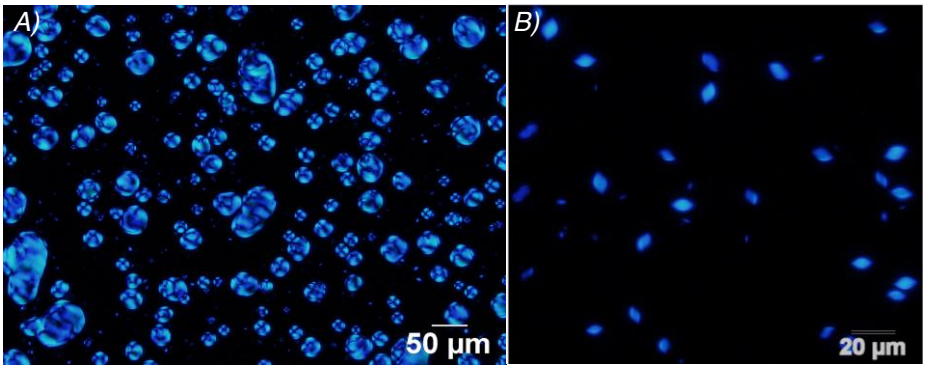


Figure 23. **9**/Water/PVP emulsion images. A) Drops and B) tactoid drops at 19.9/76.2/3.9 mass ratios.

Rheology measurements at 25 ºC, are shown in Figure 24. The solution of PVP at 4 wt% showed Newtonian behaviour (Fig. 23), which is characterised by a dynamic viscosity of 2.05 mPa·s with a standard deviation of 0.08 mPa·s (comparable with the dynamic viscosity values of 2.03 mPa·s and 2.209 mPa·s for concentrations of 3.713 wt% and 4.152 wt% found in [37]). Viscosity results are obtained as the mean value of the measured data. A big viscosity increase is observed when the dye is introduced in the solution, which corresponds to the **9**/Water/PVP emulsion formation. Emulsions also show Newtonian behaviour, which is typical of diluted emulsions.

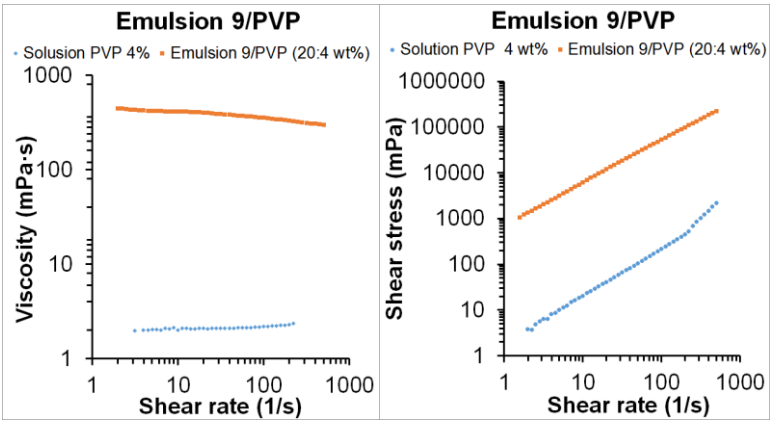


Figure 24. Rheology of PVP solution at 4 wt% and **9**/Water/PVP emulsion.

The behaviour with temperature was observed by POM. At 25 ºC drops show star-like and tactoid optical textures (Fig. 25). At 30 ºC the number of tactoids decreases and at 35 ºC they disappear, but small and big drops are still observed. A reduction of the drops size is observed when temperature increases. Also, the number of drops is reduced as temperature is increased and at 55 ºC, droplets disappear completely and the sample becomes isotropic. When the sample was cooled down again, no formation of drops or mesogenic phase was observed. This indicates that the system is metastablee. Destabilization of the Emulsion containing **9** with centrifugation was tested. Even at 5000 rpm with heat and over a long-time (more than an hour), separation in two phases was not observed. The formation of a fiber-like structure is observed under POM and no supernatant or sediment with birefringence was identified.

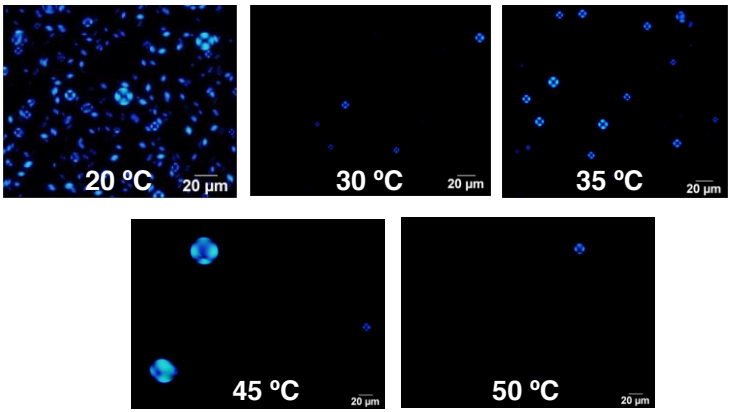


Figure 25. POM of **9**/Water/PVP emulsion at 19.9/76.2/3.9 mass ratios.

# 7. CONCLUSIONS

The first objective was to make a preliminary study to determine the capacity for chromonic liquid crystal formation in the 9 studied dyes, which was achieved for 7 of them:

- Acid red 27, Alcian blue acetate salt, Neutral red acetate and Congo red showed chromonic behaviour, but they may need to be purified to obtain single phase samples.
- The ion exchange for acetate did not affect the formation of mesophases in Alcian blue and Neutral red.
- AzBTs and Indocarbocyanine sodium salt showed the formation of insoluble solid crystals due to steric factor or counter ion effect.
- Pinacyanol acetate features a cromonic nematic phase ($N_c$ phase) at 3 wt%, which is formed by hollow columns.
- Nickel (II) phthalocyanine tetra-sulfonic acid behaves as a chromonic system.
- Alcian blue chloride salt features a nematic phase at 1 wt%.

Further characterization of the chromonic phases was carried out for nickel (II) phthalocyanine tetra-sulfonic acid, where:

- A $N_c$ phase was found between 20-25 wt%. Aggregates in this phase consisted in columns formed by one molecule in the cross-section with a diameter of 1.1 nm. The columns are formed by the stacking of 3 to 6 molecules.
- The chromonic hexagonal phase (M phase) was found at 29 wt%, which was formed by columns with an approximate diameter of 0.6 nm, which corresponds to the phthalocyanine core.

These mesophases were highly dependent on temperature and concentration. The difference in the diameter between the $N_c$ and M phases could be due to the contribution of the charged peripheral groups (including hydration), which are not considered in the calculations for the M phase. The other dyes were not well characterized due to solubility problems.

The chromonic confinement in stable emulsions, as second objective, was achieved for two different systems. These consisted in the confinement of Pinacyanol acetate and nickel (II) phthalocyanine tetra-sulfonic acid, where:

- A formulation of water-in-oil stable emulsion was produced with a solution of 3 wt% of Pinacyanol acetate/polydimethylsiloxane, vinyldimethylsiloxy terminated 0.7 cSt/KF6104, at mass ratio of 4/79/17. This showed a Newtonian rheological behaviour. Dilution of the emulsion did not change its stability. Emulsion drops presented size polydispersity with values above 2 μm.
- A highly stable water-in-water emulsion was produced by mixing nickel (II) phthalocyanine tetra-sulfonic acid/water/polyvinylpirrolydone K30, at a mass ratio of 20/76/4. The emulsion showed a Newtonian behaviour and is not formed back when cooled from the isotropic state. Emulsion drops presented size polydispersity with values above 1 μm.

The formation of optical textures representative of the chromonic confinement were observed in the stable systems, as start-like and tactoid forms. Other surfactants (Span 80) and oils (Isopropyl myristate and Squalene) did not generate stable emulsions in any of the studied compositions, but in some cases birefringent drops were observed. Formulation with polyethylene glycol did not result in the formation of stable emulsions for any of the studied dyes. Pinacyanol acetate and polyvinylpirrolydone K30 did not formed any water-in-water emulsion.

# 8. REFERENCES AND NOTES


1. Van Der Asdonk P, Kouwer PHJ. Liquid crystal templating as an approach to spatially and temporally organise soft matter. Chem Soc Rev. 2017;46(19):5935–49.
2. Collings PJ, Hird M. Introduction to liquid crystals chemistry and physics. London: Taylor & Francis; 1997.
3. Tam-Chang SW, Huang L. Chromonic liquid crystals: Properties and applications as functional materials. Chem Commun. 2008;(17):1957–67.
4. Priestley EB. Liquid Crystal Mesophases. In: Priestley EB, Wojtowicz PJ, Sheng P, editors. Introduction to liquid crystals. 1st ed. New York and London: Plenum Press; 1975. 1–12 p.
5. Pikin S, Blinov L. Fisica al alcance de todos: Cristales líquidos. Hayka: Editorial Mir Moscu; 1985. 1–54 p.
6. Lydon J. Chromonic review. J Matter Chem. 2010;20:10071–99.
7. Lydon J. Chromonic liquid crystalline phases. Liq Cryst. 2011;38(11–12):1663–81.
8. Collings PJ, Dickinson A, Smith E. Molecular aggregation and chromonic liquid crystals. Liq Cryst. 2010;37(6–7):701–10.
9. Lydon J. Chromonics. In: Demus D, Goodby JW, Gray GW, Spiess H-W, Vill V, editors. Handbook of liquid Crystals Low Molecular Weight Liquid Crystals II. New York, Weinheim, Chichester, Brisbane, Singapore, Toronto: Wiley-VCH; 1998. 981–1006 p.
10. Kustanovich I, Poupko R, Zimmermann H, Luz Z, Labes MM. Lyomesophases of the diethylammonium flufenamate-water system studied by deuterium NMR spectroscopy. J Am Chem Soc. 1985;107(12):3494–501.
11. Harrison WJ, Mateer DL, Tiddy GJT. J-aggregates and liquid crystal structures of cyanine dyes. Faraday Discuss. 1996;104:139–54.
12. Harrison WJ, Mateer DL, Tiddy GJT. Liquid-Crystalline J-Aggregates Formed by Aqueous Ionic Cyanine Dyes. J Phys Chem. 1996;100(6):2310–21.
13. Tiddy GJT, Mateer DL, Ormerod AP, Harrison WJ, Edwards DJ. Highly ordered aggregates in dilute dye-water systems. Langmuir. 1995;11(2):390–3.

14. Glatter O, Kratky O. Small Angle X-ray Scattering. London: Academic Press; 1982. 1–17 p.

15. Estelrich i Latràs J. Dispersions col·loïdals. Barcelona: Edicions Universitat de Barcelona; 2004.

16. Esquena J. Water-in-water (W/W) emulsions. Curr Opin Colloid Interface Sci. 2016;25:109–19.

17. Nicolai T, Murray B. Particle stabilized water in water emulsions. Food Hydrocoll. 2017;68:157–63.

18. Iqbal M, Tao Y, Xie S, Zhu Y, Chen D, Wang X, et al. Aqueous two-phase system (ATPS): an overview and advances in its applications. Biol Proced Online. 2016 Dec 28;18(1):18.

19. Jeong J, Davidson ZS, Collings PJ, Lubensky TC, Yodh AG. Chiral symmetry breaking and surface faceting in chromonic liquid crystal droplets with giant elastic anisotropy. Proc Natl Acad Sci. 2014;111(5):1742–7.

20. Simon KA, Sejwal P, Gerecht RB, Luk Y-Y. Water-in-Water Emulsions Stabilized by Non-Amphiphilic Interactions: Polymer-Dispersed Lyotropic Liquid Crystals. Langmuir. 2007;23(3):1453–8.

21. Tortora L, Park H-S, Kang S-W, Savaryn V, Hong S-H, Kaznatcheev K, et al. Self-assembly, condensation, and order in aqueous lyotropic chromonic liquid crystals crowded with additives. Soft Matter. 2010;6(17):4157.

22. Harris KR. Temperature and Pressure Dependence of the Viscosities of 2-Ethylhexyl Benzoate, Bis(2-ethylhexyl) Phthalate, 2,6,10,15,19,23-Hexamethyltetracosane (Squalane), and Diisodecyl Phthalate. J Chem Eng Data. 2009;54(9):2729–38.

23. Frank J, Elewa M, M. Said M, El Shihawy HA, El-Sadek M, Müller D, et al. Synthesis, Characterization, and Nanoencapsulation of Tetrathiatriarylmethyl and Tetrachlorotriarylmethyl (Trityl) Radical Derivatives—A Study To Advance Their Applicability as in Vivo EPR Oxygen Sensors. J Org Chem. 2015;80(13):6754–66.

24. Zhang X, Chen Y, Liu J, Zhao C, Zhang H. Investigation on the Structure of Water/AOT/IPM/Alcohols Reverse Micelles by Conductivity, Dynamic Light Scattering, and Small Angle X-ray Scattering. J Phys Chem B. 2012;116(12):3723–34.

25. Guan Y, Antonietti M, Faul CF. Ionic Self-Assembly of Dye−Surfactant Complexes: Influence of Tail Lengths and Dye Architecture on the Phase Morphology. Langmuir. 2002;18(15):5939–45.

26. Konieczny, L. The use of Congo Red as a lyotropic liquid crystal to carry stains in a

model immunotargeting system-microscopic studies. Folia Histochem Cytobiol. 1997;35(4):203–10.

27. Vasilevskaya AS, Generalova E V, Sonin AS. Chromonic mesophases. Russ Chem Rev. 1989 Sep 30;58(9):904–16.

28. Halls JE, Bourne RW, Wright KJ, Partington LI, Tamba MG, Zhou Y, et al. Electrochemistry of organometallic lyotropic chromonic liquid crystals. Electrochem commun. 2012;19:50–4.

29. McMurry J. Organic Chemistry. 8th ed. México: Cengage Learning; 2012. A-8.

30. Korolev VP. Hydration numbers and bulk properties of NH 4+ , Cl–, and NO 3- ions in solution at 298.15 K: Concentration dependence. J Struct Chem. 2016;57(1):135–9.

31. Rayner-Canham G. Química inorgánica descriptiva. México [etc.]: Pearson Educación; 2000. 93–94, A-3 p.

32. Rodríguez C, Torres CA, Tiddy GJT. Chromonic Liquid Crystalline Phases of Pinacyanol Acetate: Characterization and Use as Templates for the Preparation of Mesoporous Silica Nanofibers. Langmuir. 2011;27(6):3067–73.

33. Kunieda, H. Effect of oil on the surfactant molecular curvatures in liquid crystals. J Phys Chem B. 1998;102(5):831–8.

34. Chemistry RS. ChemSpider: Phtalocyanine [Internet]. 2015 [cited 2019 Apr 14]. Available from: http://www.chemspider.com/Chemical-Structure.4445497.html

35. Wang Y, Wu K, Kröger J, Berndt R. Review Article: Structures of phthalocyanine molecules on surfaces studied by STM. AIP Adv. 2012;2(4):041402.

36. Kohlbrecher J (Paul SIL for NS (LNS)), Bressler I (Paul SIL for NS (LNS)). SASfit: A program for fitting simple structural models to small angle scattering data. Villigen, Switzerland; 2018.

37. Bai T-C, Huang C-G, Yao W-W, Zhu C-W. Viscosity B-coefficients and activation free energy of viscous flow for hexanedioic acid in aqueous polyvinylpyrrolidone solution. Fluid Phase Equilib. 2005;232(1–2):171–81.

# 9. ACRONYMS

**C**

| | |
|---|---|
| Concentration | ([C]) |
| Chromonic hexagonal phase | (M phase) |
| Chromonic nematic phase | ($N_c$ phase) |

**D**

| | |
|---|---|
| Disodium cromoglicate | (DSCG) |

**H**

| | |
|---|---|
| Herringbone defect texture | ($M^{Hb}$) |
| Hexagonal Discotic phase | ($Col_h$) |
| Hexagonal Lyotropic phase | ($H_1$) |
| Hydrophile-Lipophile Balance | (HLB) |
| Hypermer 2296 | (Hypermer) |

**I**

| | |
|---|---|
| Isopropyl Myristate | (ISP) |
| Isotropic | (I) |

**L**

| | |
|---|---|
| Liquid Crystal | (LC) |
| Lyotropic Chromonic Liquid Crystal | (LCLC) |
| Lyotropic Chromonic Liquid Crystal/Oil/Surfactant | (LCLC/O/S) |
| Lyotropic Chromonic Liquid Crystal/Water/Polymer | (LCLC/W/P) |

**N**

| | |
|---|---|
| Nematic phase | (N phase) |
| Nematic Discotic phase | ($N_{Col}$) |
| Nematic and isotropic biphasic region | (N+I) |
| Nematic and M biphasic region | (N+M) |

**O**

| | |
|---|---|
| Oil-in-water | (O/W) |

**P**

| | |
|---|---|
| Polarized Optical Microscope | (POM) |
| Polydimethylsiloxane 0.7 cSt | (PDMS 0.7) |
| Polydimethylsiloxane 200 cSt | (PDMS 200) |
| Polyethylene glycol | (PEG) |
| Polyvinylpirrolydone | (PVP) |

**S**

| | |
|---|---|
| Scattering vector | ($q$) |
| Schlieren defect texture | ($N^{Sc}$) |
| Small Angle X Ray Scattering | (SAXS) |
| Smectic | (S) |
| Smectic A | ($S_A$) |
| Smectic B | ($S_B$) |
| Smectic E | ($S_E$) |
| Sunset Yellow | (SSY) |

**T**

| | |
|---|---|
| Temperature | (T) |

**W**

| | |
|---|---|
| Water-in-oil | (W/O) |
| Water-in-water | (W/W) |
| Weight percentage | (wt%) |

# APPENDICES

# APPENDIX 1: DYES ADDITIONAL INFORMATION

| Name | IUPAC Name |
|---|---|
| **Disodium cromoglicate** | 5-[3-(2-carboxylato-4-oxochromen-5-yl)oxy-2-hydroxypropoxy]-4-oxochromene-2-carboxylate disodium salt. |
| **Sunset yellow** | 6-hydroxy-5-[(4-sulfophenyl) azo]-2-naphthalenesulfonate disodium salt. |
| **Acid red 27** | (4E)-3-oxo-4-[(4-sulfonato-1-naphthyl)hydrazono]naphthalene-2,7-disulfonate trisodium salt. |
| **Indocarbocyanine sodium salt** | 3,3,3',3'-tetramethyl-1,1'-bis(4-sulfobutyl)-indocarbocyanine sodium salt. |
| **Congo red** | 4-amino-3-[[4-[4-[(1-amino-4-sulfonatonaphthalen-2-yl) diazenyl] phenyl] phenyl] diazenyl] naphthalene-1-sulfonate disodium salt. |
| **Neutral red** | 3-Amino-7-dimethylamino-2-methylphenazine hydrochloride |
| **Alcian blue** | A, B, C, D-tetrakis-(pyridiniomethyl) Cu(II) phthalocyanine chloride |
| **Pinacyanol acetate** | 1,1'-Diethyl-2,2'-carbocyanine chloride, 2,2'-Trimethinequinocyanine acetate |
| **Nickel (II) phthalocyanine tetra-sulfonic acid** | Nickel (II) phtalocyanine-tetra-sulfonic acid tetrasodium salt |
| **AzBTs** | 2,2'-Azinobis (3-ethylbenzothiazoline-6-sulfonic Acid Ammonium salt) |

# APPENDIX 2: CHEMICALS.

## APPENDIX 2.1. SURFACTANTS AND POLYMERS.

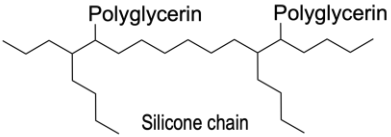


Plyglyceryl-3 Polydimethylsiloxyethyl dimethicone

**KF6104**

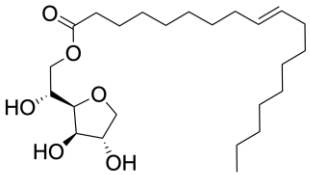

$C_{24}H_{44}O_6$

(Z)-Sorbitan mono-9-octadecenoate

**Span 80**

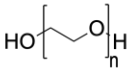

$H(C_2H_4O)_nOH$

**Polyethylene glicol 4000**

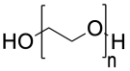

$H(C_2H_4O)_nOH$

**Polyethylene glicol 10000**

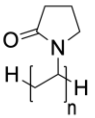

$(C_6H_{11}NO)_n$

**Polyvinylpirrolydone K30**

## APPENDIX 2.2. OILS.

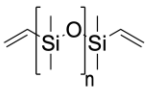

$C_{6+2n}H_{12+6n}O_nSi_{1+n}$

Molecular weight aprox. 186 g/mol

Polydimethilsiloxane, vinyldimethylsiloxy terminated; viscosity 0,7 cSt

**Polydimethilsiloxane 0,7 cSt**

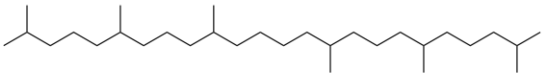

$C_{30}H_{62}$

Molecular weight 422,81 g/mol

2,6,15,19,23-Hexamethyltetracosane

**Squalane**

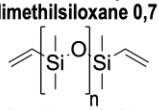

$C_{6+2n}H_{12+6n}O_nSi_{1+n}$

Molecular weight aprox. 9400 g/mol

Polydimethilsiloxane, vinyldimethylsiloxy terminated; viscosity 200 cSt

**Polydimethilsiloxane 200 cSt**

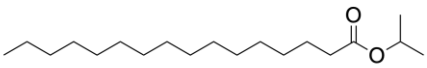

$C_{19}H_{38}O_2$

Molecular weight: 298,51 g/mol

Propan-2-yl tetradecanoate

**Isopropyl Myristate**